

# TIME DOMAIN SIMULATIONS OF DYNAMIC RIVER NETWORKS

Tony Lange <sup>\*</sup>, M.K. Banda<sup>†</sup> and J.-M. T. Ngnotchouye <sup>‡</sup>

## Abstract

The problem of simulating a river network is considered. A river network is considered to comprise of rivers, dams/lakes as well as weirs. We suggest a numerical approach with specific features that enable the correct representation of these assets. For each river the flow of water is described by the shallow water equations which is a system of hyperbolic partial differential equations and at the junctions of the rivers, suitable coupling conditions, viewed as interior boundary conditions are used to couple the dynamics. A different model for the dams is also presented. Numerical test cases are presented which show that the model is able to reproduce the expected dynamics of the system. Other aspects of the modelling such as rainfall, run-off, overflow/flooding, evaporation, absorption/seepage, bed-slopes, bed friction have not been incorporated in the model due to their specific nature.

## 1 Introduction

In this article we consider a time domain simulation of dynamics of river networks. This can also be understood as simulation of the time evolution of river networks. The need to model and simulate a water network arises due

---

<sup>\*</sup>Optin, P.O. Box 44207, Linden 2104, South Africa. *e-mail: tony@optin.co.za*

<sup>†</sup>School of Computational and Applied Mathematics, University of the Witwatersrand, Johannesburg, Private Bag 3, Wits 2050, South Africa. *e-mail: Mapundi.Banda@wits.ac.za*

<sup>‡</sup>School of Mathematical Sciences, University of KwaZulu-Natal, Private Bag X03, Scottsville 3209, South Africa. *e-mail: 207521833@ukzn.ac.za*

to the fact that monitoring and prediction of the dynamics of rivers play an important role in the predictive abilities of decision-makers. These take the form of monitoring and predicting water levels in order to optimize water supply, eradicating or reducing the impacts of catastrophes due to flooding rivers, emptying of reservoirs, or breaking of dams. The main features of the river flow network to be considered may include the following:

- modelling of the river flow;
- modelling of branched river networks;
- modelling of a reservoir or a storage basin.

In this work, we employ a network approach based on one-dimensional models. This is a result of the fact that on a large scale, the flow is a one-dimensional phenomenon. Thus topographical maps can be transformed to network graphs. The elements of such a network graph include single river reaches as well as dams which are edges of the graph connected by vertices that are intersections of rivers as well as weirs. The flow in the rivers is described mathematically by the application of the shallow water equations. This model, which was introduced by A.J.C de Saint Venant in 1871, is widely used to model flows in rivers and coastal areas. For a branched network, we describe and implement some coupling mechanisms at the intersection of three rivers, at the confluence of a big river and a tributary, and at a weir (or a river dam). These coupling mechanisms are some algebraic equations representing some interior boundary conditions at the intersection point [12] which are motivated by physical considerations. The dynamics of the volume of water in a reservoir or a storage basin is modelled by a function of the flux of water into and out of the reservoir. This can be described by a system of differential equations. Such modelling also allows a detailed focus on parts of the river that could be of special interest.

The numerical approach we have applied to approximate the river flow is an upwind scheme. This has the advantage of simplicity and robustness. Unfortunately, it does introduce significant numerical diffusion hence steep flow gradients are not sharply resolved. In a network it is believed that such detail may not be very critical. Indeed, an extension to more accurate schemes is feasible if the need for more detailed focus arises. Such high resolution schemes have been extensively discussed in the literature and we list some publications below [11, 13, 6, 7]. Such schemes are nonlinear and

as a consequence are not trivial to implement and more expensive than first-order schemes. Sharper resolutions for upwind schemes can be attained by refining the spatial grid used in numerical approximations.

The rest of this article is organized as follows. In Section 2, we introduce the formulation of the shallow water equations used to model the flow of water in the rivers. The properties of this system of conservation laws is reviewed and some parameters describing the characteristics of the flow are introduced. In Section 3, we present the coupling conditions used at the confluence of rivers' reaches. These are mainly the continuity of the water level at the intersection and the conservation of mass of water through the junction. In Section 4, numerical schemes used to solve the flow equations and the implementation of the coupling mechanisms are discussed. Some numerical examples are used to demonstrate the robustness and the efficiency of this approach.

## 2 Modelling the dynamics of a river

An open channel flow is a flow system in which the top surface of the fluid is exposed to the atmosphere. Rivers and dams fall under this definition. In this section, we will present the modelling of the rivers and dams and then define the coupling conditions necessary for a network.

### 2.1 The shallow water model

To model the flow of water in a river the conservation of mass and momentum of the flow is considered. The model is derived from the depth averaging of the incompressible flow models. In general, to model the conservation of mass along the flow direction in a channel of arbitrary cross-section one considers the cross-sectional area of water  $A$  [ $L^2$ ], at time  $t$ [s] and point  $x$  [ $L$ ] as presented in Figure 1. If a small section of a river is considered then the rate of change of the cross-sectional area of the river is a result of the gradient of the total volume flow rate also known as discharge  $Q$ , in that section of the river. This might be balanced by other mass source or sink terms  $S_m$  (for example, rainfall, evaporation, seepage, runoff) to give equation (1a) in which  $\partial_t$  is a partial derivative with respect to time and  $\partial_x$  is a partial derivative with respect to space (distance). One also refers to  $S_m$  [ $L^2/T$ ] as the volume flux per unit length into the stream. Equation (1b) describes

the balance of momentum, here represented by the discharge  $Q$  : the rate of change of discharge depends on the flow of momentum,  $\frac{Q^2}{A}$ , the hydrostatic pressure term  $I_1$ , the effect of the forces exerted by the channel walls on the flow  $I_2$ , the bottom slope of the channel  $S_0$ , and the frictional forces at the bottom  $S_f$ :

$$\partial_t A + \partial_x Q = S_m, \quad (1a)$$

$$\partial_t Q + \partial_x \left( \frac{Q^2}{A} + gI_1 \right) = g(I_2 + A(S_0 - S_f)). \quad (1b)$$

This is a conservative formulation in which  $A(x, t)$  is the wetted cross-section area:

$$A(x, t) = \int_{B(x)}^{B(x)+h(x,t)} \sigma(x, y) dy.$$

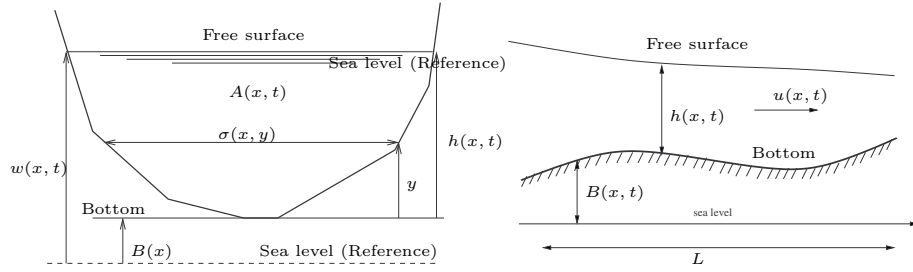


Figure 1: Cross section at  $x$  (left) and side view of the river (right)

In (1)(see Figure 1),  $x$  is the longitudinal position in the river. The river is assumed to be of length  $L$  and  $t$  is time. The hydrostatic pressure term,  $I_1 = I_1(x, h)$  is defined as

$$I_1 = \int_{B(x)}^{B(x)+h} (h - y) \sigma(x, y) dy, \quad (2)$$

where  $\sigma$  is the channel breadth,  $h$  the channel height and  $y$  the coordinate in the vertical direction. On the other hand  $I_2 = I_2(x, h)$  is the term that accounts for the forces exerted by the channel walls at the contractions and expansions due to longitudinal width variations

$$I_2 = \int_{B(x)}^{B(x)+h} (h - y) \frac{\partial \sigma}{\partial x}(x, y) dy. \quad (3)$$

Note that  $h = h(x, t)$  is the water depth. Due to their geometric interpretation, we have that

$$\sigma(x, y) > 0 \text{ for all } x \in [0, L] \text{ and } y \geq 0. \quad (4)$$

The bottom slope  $S_0$  is given by

$$S_0 = -\frac{dB}{dx}(x) \quad (5)$$

where  $B = B(x)$  describes the bottom topography (bottom elevation) of the channel. Any erosion effects are likely to happen in a much longer time scale than the dynamics of interest in this paper.

The friction term is given as

$$S_f = -\frac{n_m^2 Q |Q|}{A^2 R^{4/3}} \quad (6)$$

where  $n_m$  is the Manning roughness coefficient, given in tables, see for example [10]; and the hydraulic radius  $R = A/P$ ,  $P$  being the wetted perimeter of the river at position  $x$ .

When the channel cross section is locally rectangular, triangular or trapezoidal, the pressure force integrals  $I_1$  and  $I_2$  can be expressed as

$$I_1 = h^2 \left( \frac{\sigma_0}{2} + \frac{hZ}{3} \right), \quad I_2 = h^2 \left( \frac{1}{2} \frac{\partial \sigma_0}{\partial x} + \frac{h}{3} Z_x \right),$$

where  $\sigma_0$  is the channel bottom width (with  $\sigma_0 = \sigma$  for a rectangular channel) and  $Z$  is the slope of the channel (vertical to horizontal). For the case of rectangular cross section, the model (1) takes the simplified form

$$\partial_t A + \partial_x Q = S_m, \quad (7a)$$

$$\partial_t Q + \partial_x \left( \frac{Q^2}{A} + \frac{1}{2} g \sigma h^2 \right) = gh \left( \frac{1}{2} h \sigma' - \sigma B' \right), \quad (7b)$$

where the prime stands for the derivative with respect to the space variable  $x$ . The convective part of the model (7), that is the model (7) with a vanishing right hand side, is strictly hyperbolic. Indeed, the Jacobian matrix of the flux function is given by

$$J = \begin{pmatrix} 0 & 1 \\ g \frac{A}{\sigma} - u^2 & 2u \end{pmatrix},$$

where  $u = Q/A$  is the stream-wise velocity of the fluid. The eigenvalues and eigenvectors are given respectively by  $\lambda_{\mp} = u \mp \sqrt{gA/\sigma}$  and  $e^{\mp} = (1, \lambda_{\mp})^T$ . Therefore when  $A/\sigma > 0$ , the system (7) is strictly hyperbolic.

Since here we assume locally rectangular channel, we have that

$$A = \sigma h \quad \text{and} \quad Q = Au = \sigma hu$$

and substituting in (7), we recover by simplifying by  $\sigma$  and assuming that  $S_m = 0$ , the usual form of the shallow water equations in terms of the water height  $h$ .

$$\begin{aligned} \partial_t h + \partial_x(hu) &= 0, \\ \partial_t(hu) + \partial_x(hu^2 + \frac{g}{2}h^2) &= -ghB'. \end{aligned} \quad (8)$$

In the rest of this article, we will be mainly interested in the water height  $w = h + B$  (see Figure 1) and the quantity  $hu$  that we denote again for clarity as  $Q = hu$ . Simple algebra helps to transform (8) to

$$\begin{aligned} \partial_t w + \partial_x(Q) &= 0, \\ \partial_t(Q) + \partial_x\left(\frac{Q^2}{w-B} + \frac{g}{2}(w-B)^2\right) &= -g(w-B)B'. \end{aligned} \quad (9)$$

It is in this form that the implementation and the simulation will be carried out later.

Since the original form of the shallow water equations [6] are derived under the assumption of a conservation of the volume of water without taking into account the effect of rain fall, evaporation and seepage, we choose the source term in the mass balance equation to account for these effects. To fix our ideas, we choose a source term that takes into account rainfall, evaporation, seepage and infiltration. This information is obtained by measurement and is given in the literature by coarse models deriving from the interpolation of data [8, 9]. The rainfall rate,  $r(t)$ , can be given by a meteorological station situated near the river. The evaporation rate,  $e(t)$  depends on the surface of the river and the weather. Seepage and infiltration rate,  $s(t)$ , depend on soil water content and groundwater resources. Putting these together, the source term is then given by

$$S_m(t) = r(t) - e(t) - s(t).$$

We finish this section by pointing out some flow behavior that arise in the simulation of rivers flow.

## 2.2 Characteristics of the flow

We briefly discuss the characteristic of the flow in open-channels. One parameter that characterizes the flow in an open channel is the Reynolds number. It is given by

$$N_R = \frac{|u|R}{\nu} \quad (10)$$

where  $u$  is the average velocity of the flow,  $R$  is the hydraulic radius and  $\nu$  is the kinematic viscosity of the fluid. Laminar flow occurs when  $N_R < 500$  and turbulent flow occurs when  $N_R > 2000$ . The transition region corresponds to the Reynolds number in the range 500 to 2000 [10]. Besides the viscosity versus inertial forces that is captured by the Reynolds number, the ratio of inertial forces to gravity forces, given by the Froude number, plays an important role in the characterization of open channel flow. It is given by

$$N_F = \frac{|u|}{\sqrt{gy_h}} \quad (11)$$

where  $y_h$ , called the hydraulic depth, is given by  $y_h = A/T$  with  $A$  being the wetted cross-section area and  $T$  being the width of the free surface of the fluid at the top of the channel.

When the Froude number is equal to 1.0, that is, when  $u = \sqrt{gy_h}$ , the flow is called a critical flow. When  $N_F < 1.0$ , the flow is subcritical (or fluvial) and the flow is dubbed supercritical (or torrential) when  $N_F > 1.0$ .

With a channel with a locally rectangular cross section, the Froude number simplifies to

$$N_F = \frac{|u|}{\sqrt{gh}},$$

where  $h$  is the water height. This expression is closely related to the eigenvalues of the flux function of the shallow water equations in this case.

## 3 Coupling of confluencing rivers

We index the rivers and the quantities associated with them by  $i \in \mathcal{I} = \{1, \dots, n\}$ . We label the locations of the end points of the canals and dams, which we shall refer to as nodes, by  $j \in \mathcal{J} = \{1, \dots, m\}$ . We distinguish between multiple nodes, indexed by  $j \in \mathcal{J}_M$ , at which various rivers come

together, and simple nodes, indexed by  $j \in \mathcal{J}_S$ , which are endpoints of a single river. For  $j \in \mathcal{J}$ , we introduce

$$\mathcal{I}_j = \{i \in \mathcal{I} : \text{the } i\text{-th river meets the } j\text{-th node}\}.$$

For each river  $i \in \mathcal{I}$ , the dynamics is described by a copy of the model (9), that is

$$\partial_t w_i + \partial_x Q_i = 0, \quad (12a)$$

$$\partial_t Q_i + \partial_x \left( \frac{Q_i^2}{w_i - B} + \frac{1}{2} g(w_i - B_i)^2 \right) = -g(w_i - B_i) B_i'. \quad (12b)$$

In (12b),  $B_i$  is the bottom elevation in channel  $i$ . We will look at different common types of intersection that are encountered in real life water networks.

### 3.1 Intersection of three rivers with the same size

Here we consider three rivers of equal strength (i.e. similar breadths and wetted cross-sectional areas) meeting at a node 1. The configuration is depicted in Figure 2.

In this case, we prescribe the Rankine-Hugoniot condition at the junction:

$$Q_3 = Q_1 + Q_2.$$

This condition simply ensures that the volume flux in reach 3 at the intersection is equal to the volume flux from reach 1 and reach 2. We also impose equal water level at the intersection, that is, we have at the junction,

$$w_3 = w_2 = w_1.$$

These conditions are physically motivated and ensure the conservation of mass of water as well as the continuity of the water height at the junction.

### 3.2 Intersection of a river and a tributary

Now we consider the confluence of a big river and a small tributary as shown in Figure 3. The width of the tributary is assumed to be very small compared to that of the main river. We are mainly interested in the influence of the tributary downstream of the main river. A loose coupling is given if the

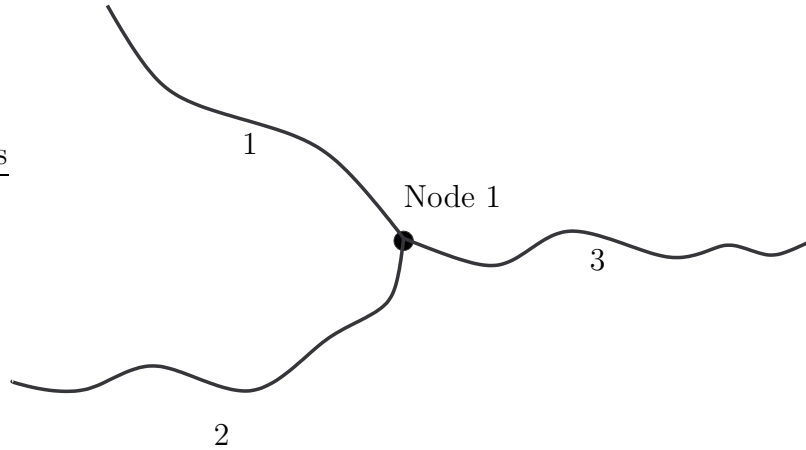


Figure 2: Junction of three rivers of equal strength.

model for the tributary can be calculated at first and the model for the main river afterwards. With this one way coupling, it is hardly possible to take into account flow information from the large river into the model of the tributary. We will assume here that the rivers are well instrumented. Precisely, we assume that there is a gauging-station located directly downstream of the relevant tributary. Therefore, the water level information  $w_g(t)$ , from the gauging-station is used for a lower boundary condition for the tributary,

$$w_1(t, \bar{x}) = w_g(t). \quad (13)$$

Once the tributary model has been run, its calculated outflow at the junction  $Q_1(t, \bar{x})$  must be considered as a lateral inflow

$$S_{m2} = \begin{cases} 0 & \text{if } x < \bar{x}, \\ Q_1(t, \bar{x})/(x - \bar{x}) & \text{if } x > \bar{x}, \end{cases}$$

to the main river after the confluent point. This ensures that the tributary affects the main river near to the junction only. Far from the junction, the effect of the tributary on the main river vanishes. For the implementation, the condition  $x = \bar{x}$  may be replaced by the more practical one  $|x - \bar{x}| < \varepsilon$  where  $\varepsilon > 0$  is a very small number.

### 3.3 Coupling of a weir and storage basin

A weir is modelled by splitting the river into a reach upstream and downstream the weir. The downstream boundary condition of the upstream reach

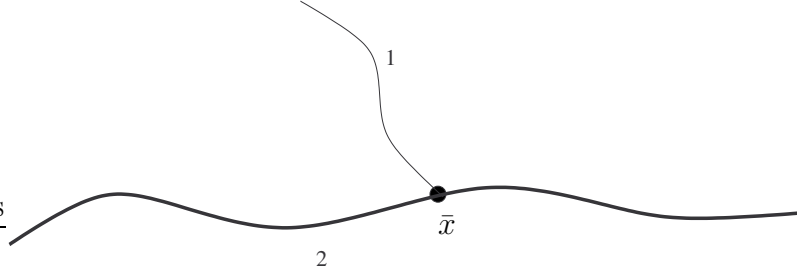


Figure 3: A river and its tributary

is given as in (13), that is

$$w_{\text{upstream}} = f(Q_{\text{upstream}}, t).$$

Some rivers are steered in a way that the water level directly upstream of the weir is practically constant over time, this translates to the new coupling condition

$$w_{\text{upstream}} = \text{constant}.$$

In any case, the upstream water level at the downstream reach needs to be smaller than the water level downstream of the upstream reach. When floods occur, this condition can be violated. Then to ensure a good resolution of the flow equation, the boundary condition at the downstream of the upstream reach needs to have the form [12]:

$$w_{\text{upstream}}(t) = \max(w_{\text{downstream}}(t), f(Q_{\text{upstream}}, t)).$$

For the discharge, we prescribe naturally the conservation of mass at the interface:

$$Q_{\text{upstream}} = Q_{\text{downstream}}.$$

The effective flow area is treated as interconnecting storage basins, for each of which the relation between storage volume and water level is known or assumed. The flow calculation between the basins is based on the continuity of volume for each basin and non-inertial flow laws between basins. Continuity of volume in a reservoir or storage basin  $j$  is expressed as [8]

$$\frac{\partial V_j}{\partial t} = \sum_{i=1}^n Q_{ij}, \quad (14)$$

where  $V_j [m^3]$  is the volume of water in the basin  $j$ ;  $n$  is the number of connections leading to basin  $j$ ,  $Q_{ij} [m^3/s]$  is the discharge from basin  $i$  to basin  $j$  or from river cross section  $i$  to basin  $j$ .

## 4 Numerical approach to approximate network dynamics

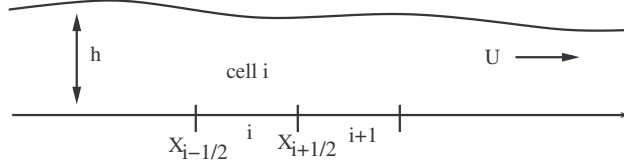


Figure 4: A finite-volume scheme discretization.

A simple discretization of the shallow water equations may follow a standard finite volume approach as shown in Figure 4. From the cell average variable

$$v_j = \frac{1}{\Delta x_j} \int_{x_{j-1/2}}^{x_{j+1/2}} v(x, t) dx$$

on the control volume  $I_j = [x_{j-1/2}, x_{j+1/2}]$  of length  $\Delta x = \Delta x_j = x_{j+1/2} - x_{j-1/2}$ , an integration of the non-homogeneous conservation law

$$\partial_t v + \partial_x f(v) = g(v)$$

over  $I_j$  leads to

$$\partial_t v_j = -\frac{1}{\Delta x_j} (f(v(x_{j+1/2}, t)) - f(v(x_{j-1/2}, t))) + \frac{1}{\Delta x_j} \int_{x_{j-1/2}}^{x_{j+1/2}} g(v) dx. \quad (15)$$

The main problem now is to recover the unknowns  $v(x, t)$  at the cell boundaries  $x_{j\pm 1/2}$  from the cell averages  $v_j$  and to approximate the source term. By using the midpoint rule for the integrals in the finite volume scheme, one easily recovers the well known finite difference method. In general, one can write the scheme (15) in the semi-discrete form

$$\frac{d}{dt} \mathbf{V}_j = -\frac{H_{j+\frac{1}{2}} - H_{j-\frac{1}{2}}}{\Delta x} + G_j \quad (16)$$

where  $H_{j+\frac{1}{2}}$  is the numerical flux and the  $G_j$  are approximations of the source term,

$$G_j \approx \frac{1}{\Delta x_j} \int_{x_{j-1/2}}^{x_{j+1/2}} g(v) dx.$$

There exists many techniques to approximate the numerical fluxes  $H_{j+\frac{1}{2}}$ . The most used are the Godunov methods which take into account the local characteristic (signal) speed at the interface of each grid cell. In its basic form, at each time level, at the interface of two neighboring cells, a Riemann problem is solved approximately for the approximate solution of the conservation law at the next time level. Examples of Godunov methods include the central-upwind method introduced in [11] that uses some non-oscillatory reconstruction of the cell average  $V_j$  via slope limiters. Many other schemes have been developed for general conservation laws and specifically for the shallow water equations [13, 6, 7]. In [7] the numerical solution of the shallow water equations was found as the kinetic limit of a relaxation system.

The shallow water equations admit steady state solutions (lake at rest, for example); therefore a numerical solution should preserve such a solution and more generally its small perturbations. A numerical scheme that satisfies this condition is known as a *well-balanced* scheme. Another desirable property for a numerical scheme for the shallow water equations is that of positivity preserving. This property ensures a correct resolution of a dry bed where the water height are very small. In this case, due to inherent numerical oscillations, the water height can take a non-positive value and can lead to non-physical solutions.

We are interested here in a simple, accurate and robust numerical method that satisfies the desirable properties described above. We adopt here the following first order approximation for the numerical fluxes [7],

$$H_{j+\frac{1}{2}} = \frac{1}{2} (f(\mathbf{V}_{j+1}) + f(\mathbf{V}_j)) - \frac{a_{j+\frac{1}{2}}}{2} (\mathbf{V}_{j+1} + \mathbf{V}_j),$$

where the local characteristic speed  $a_{j+\frac{1}{2}}$  is given by

$$a_{j+\frac{1}{2}} = \max \left( |u_{j+1}| + \sqrt{gh_{j+1}}, |u_j| + \sqrt{gh_j} \right)$$

which are approximations of the spectral radius of the Jacobian of the flux. Note that we dropped the dependence of the variable with respect to time for simplicity. For the treatment of the source term, one can adopt the upwinding method as presented in [6].

For the simulation of many intersecting rivers, we discretize the simulation time  $t_s$  according to the mesh  $t_n = n\Delta t$  for  $n = 0, 1, \dots, N$  where  $N$  satisfies  $t_s = N\Delta t$ . For each simulation step, we solve the flow equation for  $t \in [t_n, t_{n+1}]$ , we adjust the coupling and boundary condition and iterate the process. These steps are summarized in the algorithm presented in Table 1.

- Start with initial data in each river such that the coupling and boundary conditions are satisfied.
- For each simulation time interval  $[t_n, t_{n+1}]$  do the following:
- Solve the flow equation for each river for  $t \in [t_n, t_{n+1}]$ ;
  - Adjust the boundary and coupling conditions.

Table 1: Flow diagram for the computer program for the simulations.

## 5 Numerical examples and results

Now we consider some examples of water network simulation.

### 5.1 Dam-break wave simulation

We consider the dam-break problem in a rectangular channel with flat bottom  $B = 0$ . We compute the solution on a channel with length  $L = 2000$  m for time  $t = 20$  s and with initial conditions

$$\begin{aligned} u(x, 0) &= 0, \\ h(x, 0) &= \begin{cases} h_1, & x \leq 1000 \\ h_0, & x > 1000. \end{cases} \end{aligned}$$

with  $h_1 > h_0$ . We consider two cases both with  $h_1 = 10$  m: Case (a) the depth ratio  $h_0/h_1 = 0.7$  and case (b) the depth ratio  $h_0/h_1 = 0.01$ . The dam collapse at time  $t = 0$  and we have a shock wave (bore) travelling downstream, a rarefaction wave (depression wave) travelling upstream (see Figure 5).

The flow profiles are well resolved by our numerical scheme as can be seen in the result of case (b) as well. For case(a), the flow remains subcritical throughout the channel whereas for case (b) the flow is supercritical in the vicinity of the dam and subcritical far away from the dam which is situated at  $x = 1000$ , see Figure 6.

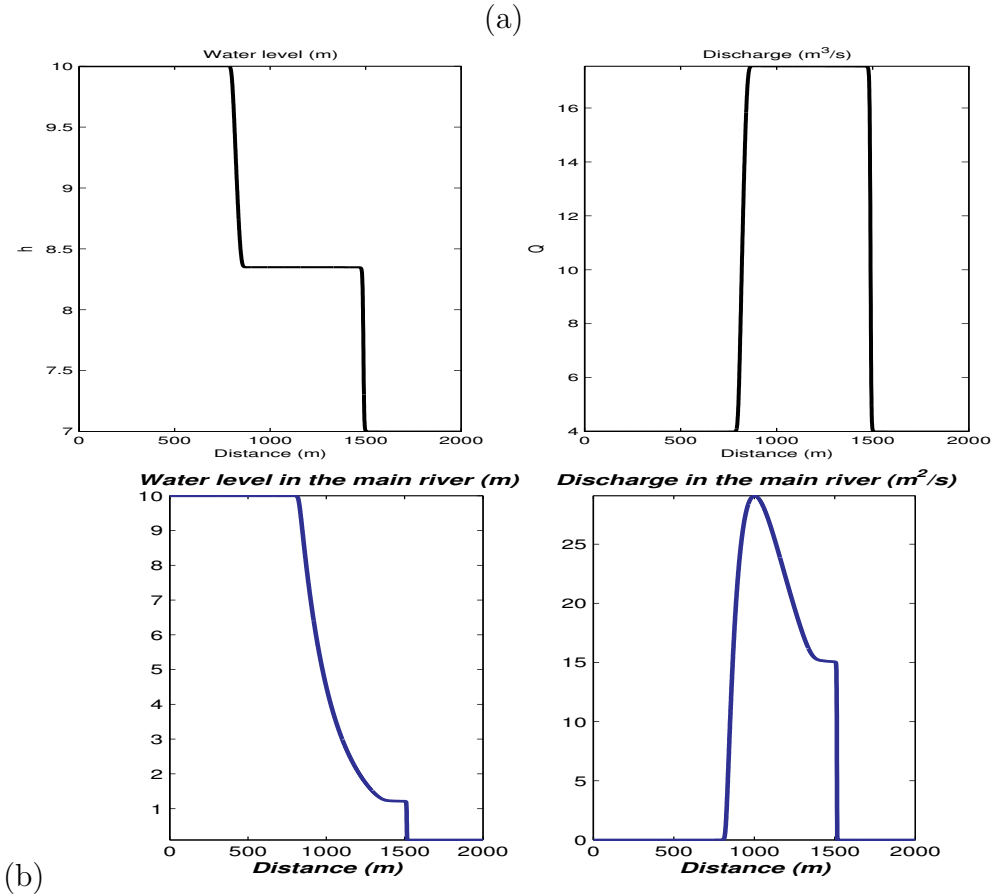


Figure 5: Water level (left) and discharge (right) for the dam-break problems.

## 5.2 Simulation of three connected channels of equal strength

The setup for this simulation is as described in Section 3.1. We consider three rivers of equal strength meeting at the same junction. The flow in each river reach is simulated by the numerical discretization of the shallow water equations as described above and the coupling conditions are introduced as interior boundary conditions. Here as in the case of the dam-break wave simulation, we assume that the rivers have a flat bottom. To drive the flow, we introduce a dam-break in each river.

We assume that the three rivers have equal length  $L = 2000\text{m}$ . The bottom topography is the same in each river i.e  $B_1 = B_2 = B_3 = 0.5\text{ m}$ . The

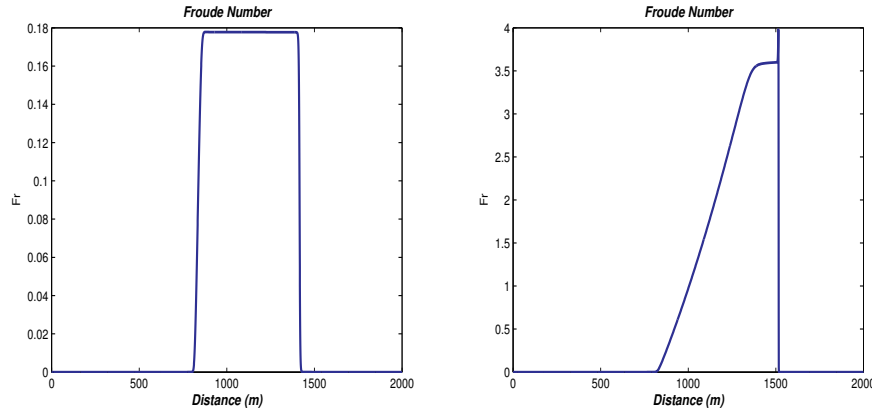


Figure 6: Froude number for the dam-break problem with the depth ratio  $h_0/h_1 = 0.7$  (left) and  $h_0/h_1 = 0.01$  (right).

initial discharge in each river is

$$Q_1 = 0.15m^3/s, \quad Q_2 = 0.45m^3/s, \quad Q_3 = 0.01m^3/s.$$

The first and second rivers are ingoing to the junction and the third river is outgoing. The intersestion is at  $x = 0$ . The results for the numerical simulation for the water levels and the discharge in each river are shown in Figure 7 and Figure 8. There appears a hydraulic jump in the first river (top) which dissipates at the intersection. The flow in the third river (bottom) is more uniform. This results from the effect of the intersection. The complex dynamics in the first river and the second river lead to a more stable and uniform flow in the third river.

### 5.3 Simulation of a main river with a tributary

Here, we use the coupling mechanism presented in Section 3.2. The width of the tributary is chosen so that it is a tenth of the width of the main river. The elevations of the river beds are assumed to be constant. We plotted in Figure 9 the water levels and the discharge in the main river where one can see that the influence of the tributary on the main river is limited to the neighborhood of the intersection point.

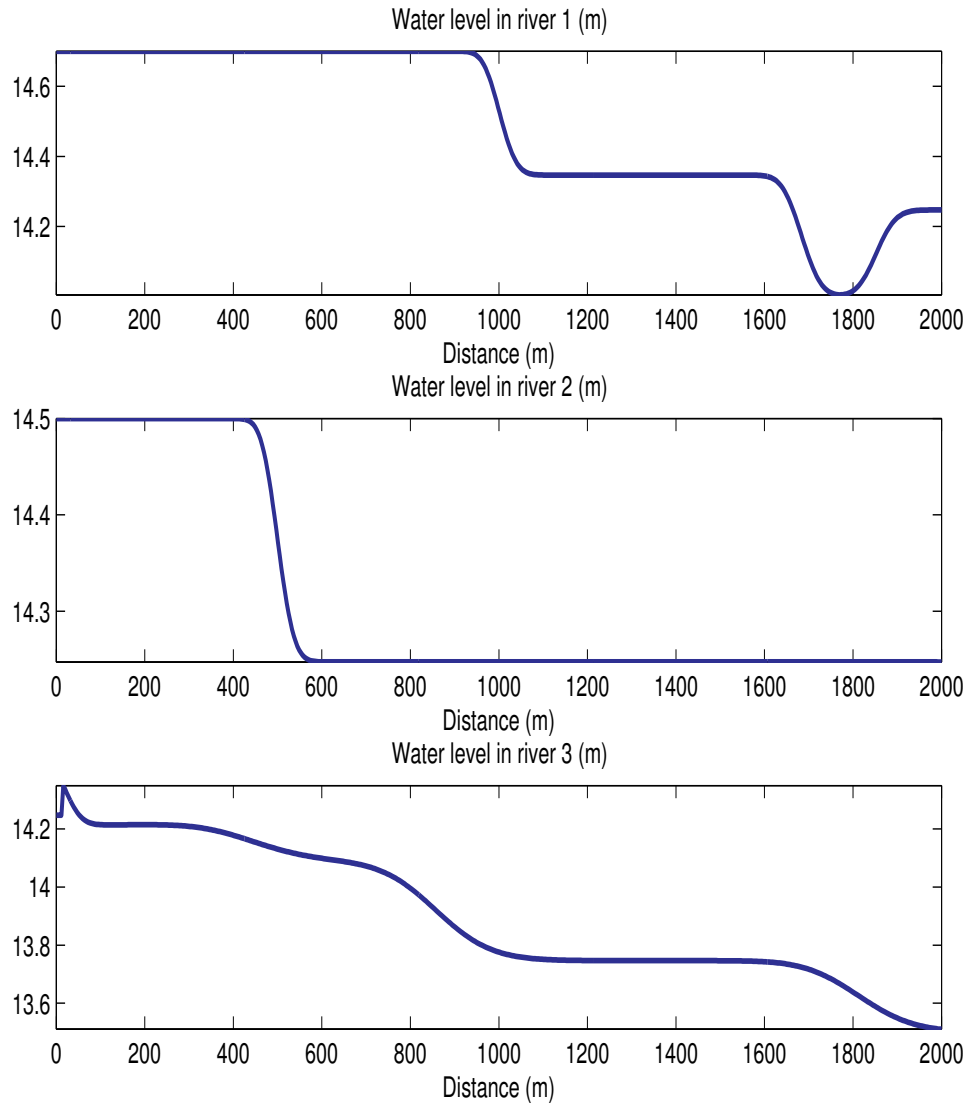


Figure 7: Water level in each river for the simulation of three rivers of same strength.

#### 5.4 Simulation of a reservoir or a storage basin

Here we consider a reservoir with arbitrary geometry. We assume that a river, say river 1, flows into the reservoir and another river, river 2, flow out of the reservoir. We are interested in the volume of the water in the reservoir.

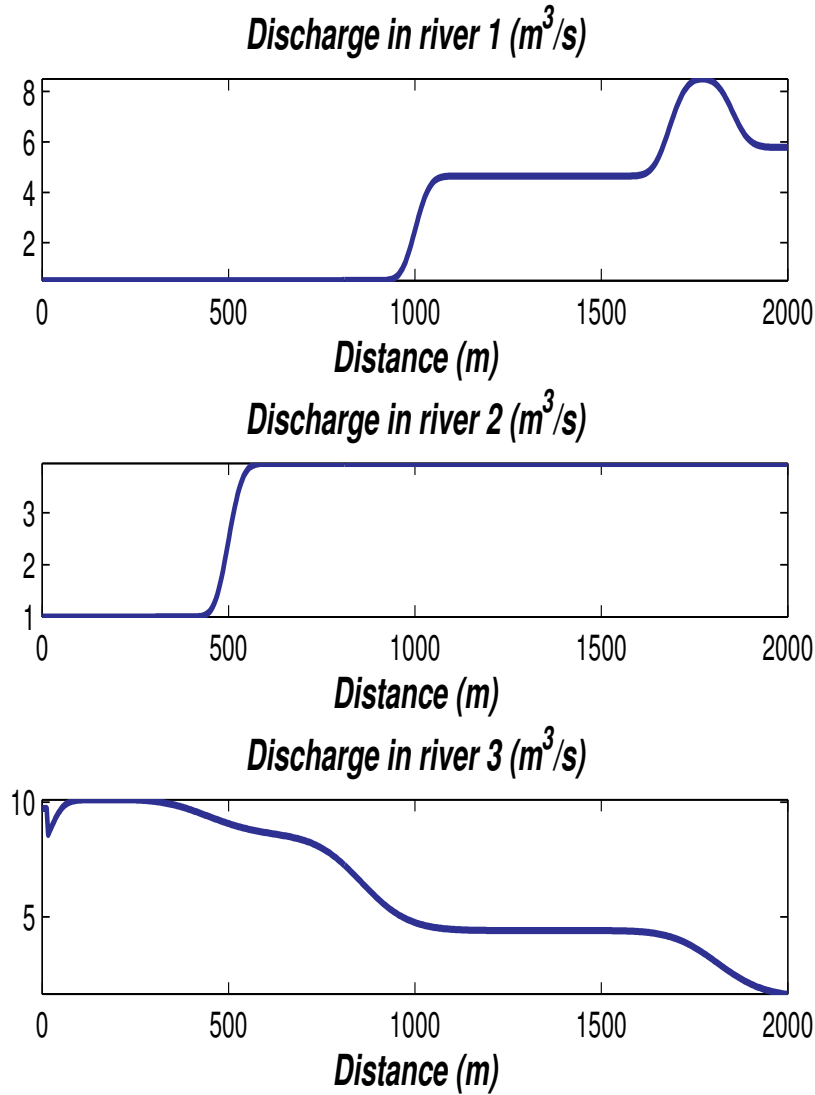


Figure 8: Discharge in each river for the simulation of three rivers of same strength.

The dynamics of that volume of water follows the model equation (14) with  $n = 2$ . Here one can assume that there is a pumping station located upstream of river 1. When the filling capacity of the reservoir is reached, the pump is switched off and therefore, the water level in river 1 and river 2 remain

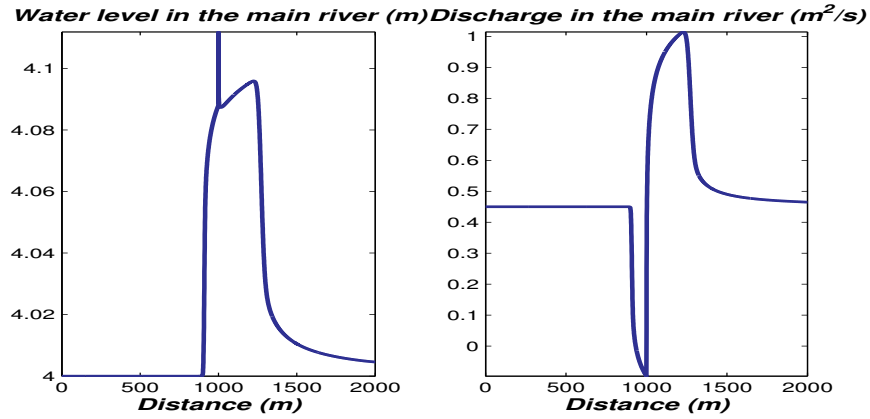


Figure 9: Water height (left) and discharge (right) in the main river. The influence of the tributary on the main river is highlighted.

constant with the same discharge, leading to a constant volume of water in the reservoir. This behavior is illustrated in our simulation presented in Figure 10. For that example, the initial volume of water in the reservoir is given by  $V_0 = 1000$  and the simulation is carried out for time length of  $t_s = 80$  seconds.

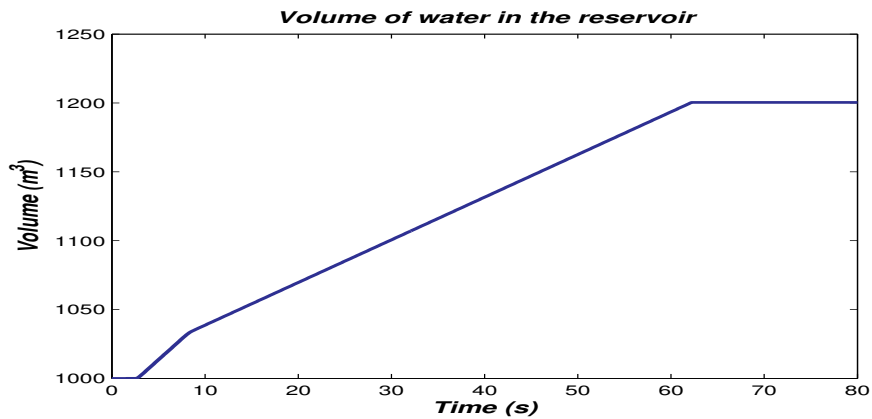


Figure 10: Evolution of the volume of water in the reservoir with time.

## 6 Concluding remarks

In this article, we have reviewed and implemented some coupling mechanisms at the junction of rivers. These comprise the analysis of dam-break wave simulations, the presence of a weir in the river or storage basins. The proposed coupling conditions for the case of three confluencing rivers are very similar to the cases studied by Colombo et al [4, 5, 3] in the case of the isothermal Euler equation and by Banda et al [2] for the multiphase drift-flux model. These authors considered the case of a network of pipes. The cases where the boundary conditions are defined by measurement with a gauging-station are more difficult to handle and can only be treated on a case by case basis [8, 9]. The simulations carried out in this work can be improved by using a more accurate numerical scheme for the flow equations. High-order schemes come at high computational costs. Nevertheless, there are quite a few suggestions on so called high resolution well-balanced schemes in the literature. The advantage of these schemes compared to what we used here is that they allow topography and breadth variations in addition to having high resolution of fluvial waves as well as preserving steady flows. The simple first-order scheme also referred to as an upwind scheme however, has the advantage of being simple and efficient and is capable of giving satisfactory results on a network, as our numerical simulations demonstrated. To close it must be pointed out that the schemes presented here are explicit in the time domain. Hence one needs to be careful of the values that are assigned to time-steps,  $\Delta t$ . The time steps will be limited by stability constraints. In addition there is no need to solve a large system of non-linear algebraic equations which would be the case if an implicit scheme was applied in time-marching. Further work will include the coupling of supercritical flow, or the case of time dependent flow beds.

## Acknowledgements

The support of the Mathematics in Industry Study Group 2008 (MISGSA 2008) is gratefully acknowledged. MKB and J-MTN express gratitude for the support from the University of KwaZulu-Natal Research Office and the NRF. The authors thank the referees for their valuable comments that helped to improve the quality of the presentation.

## References

- [1] Balbas, J and Karni, S. A central scheme for shallow water flows along channels with irregular geometry, *ESAIM: Mathematical Modelling and Numerical Analysis*, 2008, DOI: 10.1051/m2an:2008050.
- [2] Banda, M.K., Herty, M. and Ngnotchouye, J-M.T. Towards a mathematical analysis of multiphase drift-flux model in networks, Submitted (2008).
- [3] Colombo, R.M., Herty, M. and Sachers, V. On  $2 \times 2$  conservations laws at a junction, *SIAM Journal of Mathematical Analysis*, **40** (2008), 605-622.
- [4] Colombo, R.M. and Garavello, M. On the Cauchy problem for the  $p$ -system at a junction, *SIAM Journal of Mathematical Analysis*, **39** (2008), 1456-1471.
- [5] Colombo, R.M. and Garavello, M. A well posed Riemann problem for the  $p$ -system at a junction, *Networks and Heterogeneous Media*, **1**, (2006), 495–511.
- [6] Delis, A.I. Improved application of HLLC Riemann solver for the shallow water equations with source terms, *Communications in Numerical Methods in Engineering*, **19**, (2003), 59–83.
- [7] Delis, A.I. and Katsounis, Th. Relaxation schemes for the shallow water equations, *Int. J. Numer. Meth. Fluids*, **41**, (2003), 605–719.
- [8] Goutal, N. and Maurel, F. Dam break wave simulation., In: Proceedings of the 2nd Workshop on Dam-Break Wave Simulation. Technical Report EDF-DER, Report HE-43/97/016/B, Chatou, France, 1997.
- [9] Iritz, L. Rainfall input in an adaptative river flow forecast, *Hydrological Sciences-Journal des sciences hydrauliques*, **37**, (1992), 607–619.
- [10] Mott, R.L., Applied Fluid Mechanics, Pearson Prentice Hall, New Jersey, 2006.
- [11] Nessayahu, H. and Tadmor, E. Non-oscillatory central differencing for hyperbolic conservation laws, *Journal of Computational Physics*, **87**, (1990), 408–463.

- [12] Steinebach, G., Rademacher, S. Rentrop, P. and Schulz, M. Mechanism of coupling in river flow simulation systems, *Journal of Computational and Applied Mathematics*, **168**, (2004), 459–470.
- [13] Vukovic, S. and Sopta, L. Upwind schemes with exact conservation property for one-dimensional open channel flow equations, *SIAM J. Sci. Comput*, **24**, (2003), 1630–1649.